



Preliminary probabilistic assessment of the seismic response of link slab viaducts

Lucia Minnucci^a, Fabrizio Scozzese^b, Sandro Carbonari^a, Andrea Dall'Asta^b, Fabrizio Gara^a

^a Dipartimento di Ingegneria Civile, Edile e Architettura, Via Breccie Bianche, 60131 Ancona, Italy

^b Scuola di Ateneo di Architettura e Design, Università di Camerino, Viale della Rimembranza, 63100 Ascoli Piceno, Italy

Keywords: Italian bridge fragility; bridge heritage; earthquake damage; reinforced concrete infrastructures; link slab bridges.

ABSTRACT

Recent seismic events occurred in Central Italy drew the attention towards the resilience of the Italian road network, which is characterised by a significant number of old reinforced concrete bridges and viaducts. In this context, the fragility assessment of existing bridges is crucial, since their collapse or loss in functionality after earthquakes may lead to significant economic and social consequences.

As a preliminary study oriented to characterizing the fragility level of the Italian bridge heritage, this work focuses on the real case study of the Chiaravalle viaduct, located in Central Italy, which may be representative of a widespread class of reinforced concrete bridges in Italy. The viaduct is a continuous multi-span bridge consisting of precast simply supported V-shaped beams connected by a continuous upper slab. A numerical model is developed in order to capture the failure mechanisms most likely to occur for this bridge typology subjected to seismic actions. A probabilistic assessment of the seismic response of the bridge is carried out by performing multiple stripe analysis (MSA), and a preliminary interpretation of the results is provided. Future studies will be aimed to the development of fragility curves, by accounting for all the relevant demand parameters and limit states.

1 INTRODUCTION

Bridges and viaducts have a key role in transportation systems, since they represent an economic and social connection among cities and countries. The importance of such infrastructures implies the need to investigate their health as well as the resilience of their structural components after the occurrence of seismic events. In fact, failure of bridges can compromise emergency actions as well as reduce the performance of transport system for a long time (EQE 1994, EQE 1995, Kaiser et al. 2012), so bridge vulnerability is a key point in the resilience of communities and their robustness can contribute to reduce overall economic losses and fatalities.

In Italy, most of infrastructure heritage dates back to 60's and 70's (Pinto and Franchin 2010), when no specific seismic design rules were available. Among existing typologies, reinforced concrete (RC) bridges and viaducts are largely widespread on the national territory (Borzi et al.

2015). Since last seismic events occurred in Central Italy in August and October 2016, the suitability of RC bridges has become a central point for the vulnerability and the risk assessment of existing infrastructures, especially in case of Italian regions directly struck by the earthquake (Di Sarno et al. 2018). Moreover, the interest in bridge assessment has grown due to recent Italian disasters involving bridge structures (the collapse of the bridges in Lecco in 2016 and on the A14 highway in 2017, the Morandi's bridge in Genova in 2018).

The aim of this work is to provide a preliminary study on the Italian bridge heritage fragility condition, focusing on a case study of a RC bridge, the Chiaravalle viaduct, located in Central Italy. The viaduct, constituted by simply supported prestressed concrete V-shaped girders on circular piers with variable height, is realized by means of a 70's-80's construction technique, which consists in the use of simply-supported precast beams connected on the top by steel bars (links) making the slab continuous in correspondence of bearings. Under transverse and longitudinal

seismic actions this bridge typology behaves as a classical multi-span continuous bridge (Calvi 2004, Itani et al. 2004, Priestly et al. 2007, Tubaldi et al. 2012, Tubaldi and Dall'Asta 2012) but the link slab between adjacent spans represents a weakness point and a potential source of failure, to be considered in addition to classical seismic vulnerabilities generally involved in multi-span bridges (Padgett and DesRoches 2008, Kawashima 2010).

In Chapter 2, the probabilistic framework and selected analysis tools are fully described. After a brief overview on the typical vulnerabilities of link slab bridges, used to define the demand parameters of interest, the hazard scenario of the viaduct location is provided and a numerical structural model close to the real geometry of the structure is developed in order to catch potential failure mechanisms and to perform probabilistic assessment analyses. Preliminary results on different seismic intensities are provided and discussed.

2 METHODOLOGY

2.1 Probabilistic framework

A robust probabilistic framework is used in order to assess the seismic vulnerability of the bridge. In particular, Multiple Stripe Analysis (MSA) (Jalayer and Cornell 2009) is performed with the aim of providing first insights about the seismic response of the bridge and furnishing, in the next steps of this work, both the fragility curves and the demand hazard curves for all the response parameters relevant for the structural system. It is worth noting that MSA is an efficient and widely used tool for seismic risk estimation within the context of conditional probabilistic approaches. It consists of performing a number of nonlinear dynamic structural analyses at different levels of seismic intensity, the latter being expressed in terms of a proper Intensity Measure (IM) (i.e., peak ground acceleration, spectral acceleration at a given period of vibration, etc.). A probabilistic demand model can thus be built via MSA, which links the generic demand parameter D with the chosen IM through the fragility function $G_{D|IM}(d|im)$, denoting the probability of exceeding the demand value d conditional to the seismic intensity level im .

The seismic hazard is described by the function $v_{IM}(im)$, denoting the mean annual frequency (MAF) of exceeding the value im of the scalar

random variable IM , expressing the seismic intensity.

Once both the seismic hazard ($v_{IM}(im)$) and the probabilistic demand model ($G_{D|IM}(d|im)$) are available, the mean annual rate of exceedance of the demand $v_D(d)$ can be estimated (by exploiting the Total Probability Theorem) by solving the following convolution integral.

$$v_D(d) = \int_{IM} G_{D|IM}(d|im) |dv_{IM}| \quad (1)$$

2.2 Seismic hazard model

A stochastic ground motion model is used for the characterization of the seismic hazard at the site, based on two main random seismological parameters: the moment magnitude M , and the epicentral distance R . A Gutenberg-Richter recurrence law (Kramer 2003) is used to describe the magnitude-frequency relationship of the seismic source:

$$v_M(m) = 10^{(a-bm)} \quad (2)$$

where a and b are parameters characterizing the mean number of earthquakes expected from the source and the regional seismicity, respectively. The assumed recurrence law, truncated within the range of magnitudes of interest $[m_0, m_{max}]$, leads to the moment magnitude probability density function (PDF) (Kramer 2003; Au and Beck 2003; Scozzese et al. 2019):

$$f_M(m) = \beta \frac{e^{-\beta(m-m_0)}}{1 - e^{-\beta(m_{max}-m_0)}} \quad (3)$$

where $\beta = b * \log_e(10)$, m_0 and m_{max} the minimum and maximum values of magnitude expected from the source.

According to the features of the potential seismic sources in the region, the PDF of the epicentral distance is modelled as follow:

$$f_R(r) = \begin{cases} \frac{2r}{r_{max}} & \text{if } r < r_{max} \\ 0 & \text{otherwise} \end{cases} \quad (4)$$

which is obtained under the hypothesis that the source produces random earthquakes with equal likelihood anywhere within a distance from the site r_{max} . The soil condition is described by a deterministic value of the shear-wave velocity parameter V_{S30} (Boore and Joyner 1997).

The source-based ground motion model proposed in (Atkinson and Silva 2000) is used in this study, as well as in (Au and Beck 2003; Dall'Asta et al. 2017; Jalayer and Beck 2008; Scozzese et al. 2019). This model, combined with

the stochastic point source simulation method (Boore, 2003), is employed to generate ground motion time series according to the samples of M , R . Figure 1 illustrates the ground motion Fourier spectrum $A(\omega)$ and the time-envelope function $e(t)$, obtained for different earthquake moment magnitudes m (5, 6.5, 8) and a fixed epicentral distance $r=20$ km. The ground motions record-to-record variability is accounted by means of a Gaussian white noise process and a lognormal scale factor (Jalayer and Beck 2008) applied to the target Fourier spectrum.

The parameters governing the seismic scenario (M , R , a , b , V_{S30}) are defined in order to provide a IM hazard curve consistent with that from NTC 2018 for the site at hand, as thoroughly discussed in the relevant section of the paper (Section 4.2).

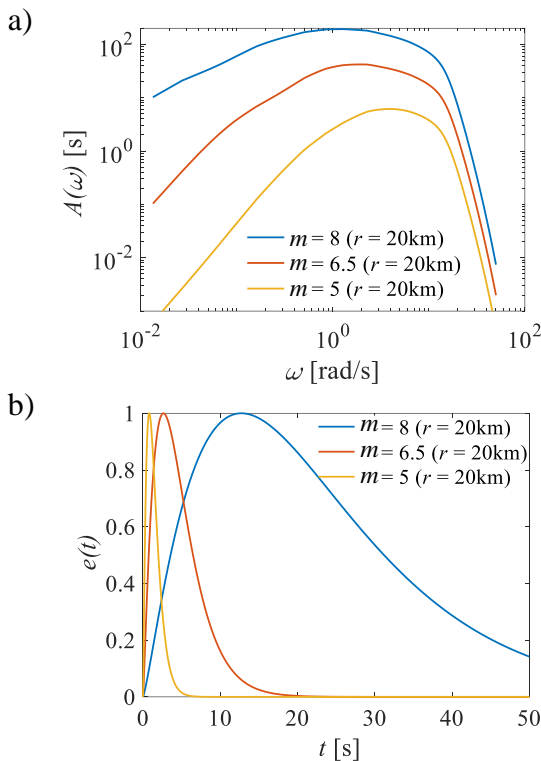


Figure 1. a) Radiation Fourier spectra and b) time-envelope functions for $r = 20$ km and different M values.

Once the seismic scenario is defined, a simulation method, called Subset Simulation (Au and Beck 2003), is adopted to generate the IM hazard curve $v_{IM}(im)$:

$$v_{IM}(im) = \bar{v}G_{IM}(im) \quad (5)$$

where \bar{v} denotes the MAF of occurrence of at least one event within the range of intensity levels of interest, and $G_{IM}(im) = P[IM > im]$ is the probability of exceedance of im , given the occurrence of an earthquake of any intensity.

3 VULNERABILITY OF LINK SLAB BRIDGES

The choice of appropriate Engineering Demand Parameters (EDPs) able to characterize the behaviour of a bridge structure and even build a prediction on the structural response for the selected bridge class is still investigated in the literature. (Karim and Yamazaki 2003) developed analytical fragility curves for highway concrete bridges considering piers as the only component describing the entire structure, referring to 4 damage states (from slight to complete) connected to the pier ductility. (Nielson and DesRoches 2007) investigated failure mechanisms in multi-span simply supported concrete girder bridges building fragility curves for piers, bearings and abutments, according to 4 limit state thresholds chosen on the basis of the timeline for the restoration of bridge functionality (FEMA 2003) with regard to the pier curvature ductility and the bearing and abutment displacement capacity. More recently, in the Italian SYNER-G project (Pitilakis 2011) three EDPs have been selected to characterize the fragility of prestressed concrete box-girder bridges, i.e. rotation of piers, shear force on piers, displacement of bearings, for two limit states, yielding and collapse. Finally, (Borzi et al. 2015) proposed the same EDPs and LSs of the SYNER-G framework to provide seismic risk maps on the Italian territory.

Link Slab (LS) bridges represent a widespread bridge class on Italian highways and road network, consisting in simply-supported beams, realized in reinforced or pre-stressed concrete girders, linked at the slab level by means of steel bars positioned in correspondence of bearings to make the existing slab continuous. The advantage of links on expansion joints consists in a lower vulnerability to wear from debris and atmospheric agents. In particular, water leaking through the joints is a major cause for the deterioration of bridge girder bearings and supporting structures, while debris accumulation in the joints restrains deck expansion and causes damage to the bridge. Furthermore, joints are expensive to install and maintain. An example of link connection is illustrated in Figure 2.

The effectiveness of link slabs as a retrofit intervention in presence of live and thermal loads, has been investigated in the literature (Caner and Zia 1998, Caner et al. 2002, Sevgili and Caner, 2009), but no probabilistic approach useful to the fragility and risk evaluation of such bridge typology has been employed yet. The presence of links represents a vulnerability source for the entire structure that must be fully investigated.

As a preliminary study of LS bridge class, in this work three main EDPs have been selected: the pier chord rotation θ , concerning the ductile mechanism of the pier, the pier base shear V_b , concerning the brittle failure, and the maximum stress on the steel bars σ_{bar} . The latter allows the detection of the stress state, the damage and eventually the failure of the girder due to transverse bending and longitudinal axial load, which is a characteristic aspect of the LS bridges.

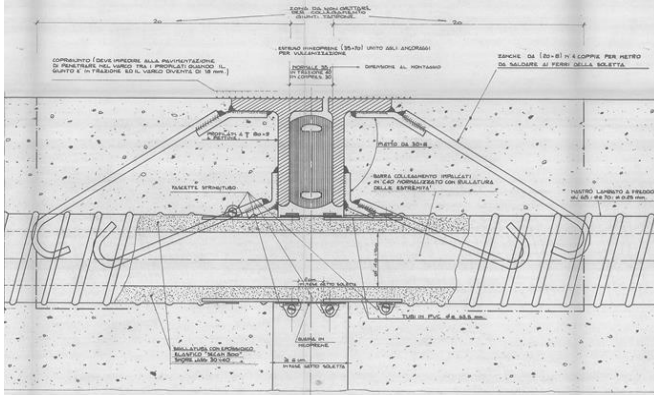


Figure 2. Detail of the joining elements between the decks.

4 APPLICATION

4.1 Case study

The Chiaravalle Viaduct is located in Falconara Marittima (AN), in a strategic position as a part of the road junction connecting the road SS76 and the highway A14 to the Falconara airport, as illustrated in Figure 3 and Figure 4.

The viaduct is 875 m long, composed of a 12.1 m wide bridge deck on 31 spans of 26.0 m length each. The bridge deck is formed by a cast on site slab on three simply supported V-shape girder beams in prestressed concrete (Figure 5).



Figure 3. Inclusion of the bridge in the existing road network.

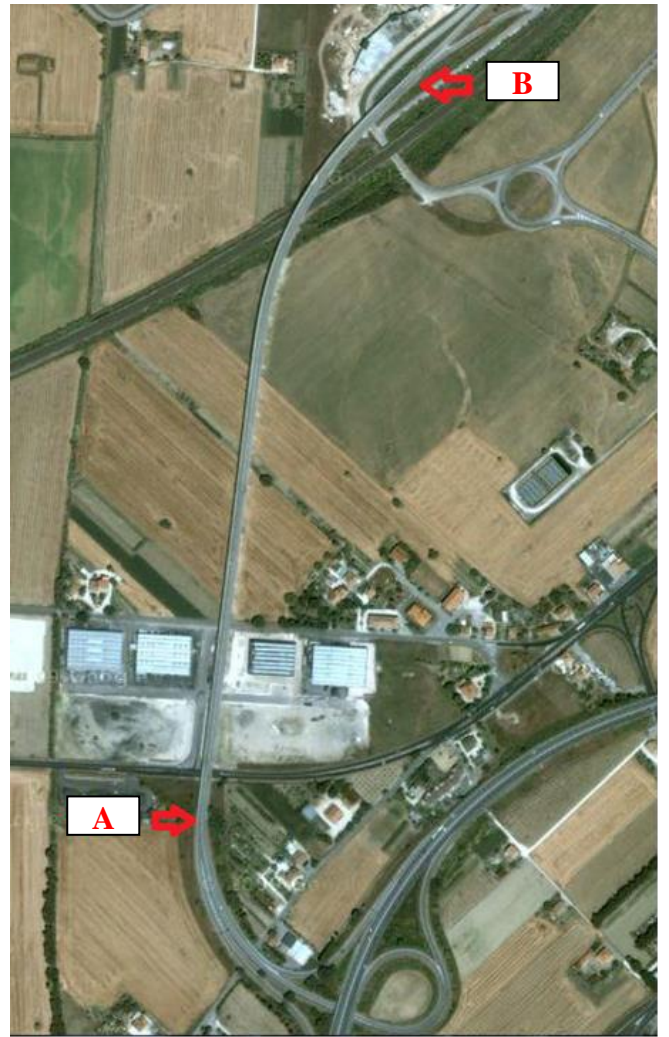


Figure 4. Aerial view of the viaduct with indication of abutments.

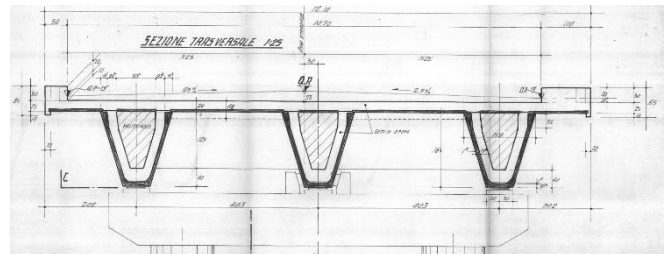


Figure 5. Cross section of the Chiaravalle viaduct.

Spans present connections at the slab level realized through so called “kinematic links”. Links are constituted by bar groups of $\text{Ø}40$ or 50 mm in a variable number from 3 to 7, as depicted in Figure 6. Each span rests on 6 steel-teflon bearings, with multi- or uni-directional transverse or longitudinal enabled movements. An example of bearing disposition under the girder beams is illustrated in Figure 7.

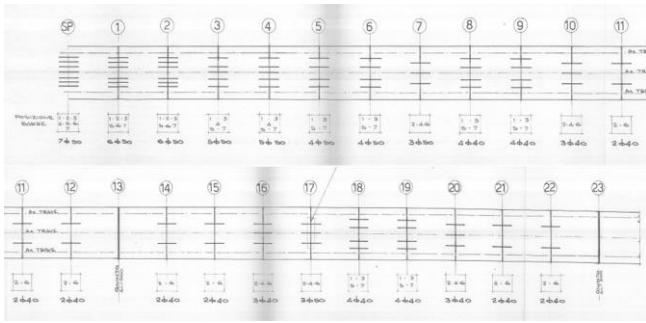


Figure 6. Location of link bars from abutment A to pier 23.

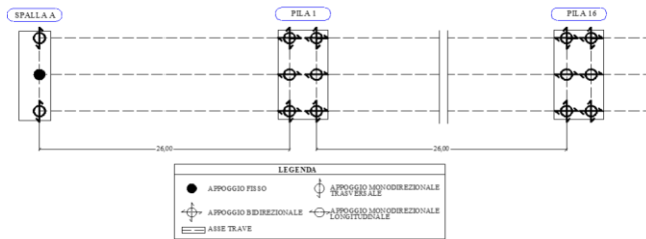


Figure 7. Bearing scheme from abutment A to pier 16.

Piers, located at a distance of 27.5 m from each other, are constituted by a RC two-columns frame with full circular section and a parallelepiped cap on the top, excepting for piers 17, 24 and 25, made up of rectangular walls. The height of the piers varies from 5.5 m to 9.5 m toward abutment B, while the circular section maintains the same characteristics for the entire bridge. Expansion joints are located in correspondence of piers 13 and 23. A prospective view of the bridge is represented in Figure 8.



Figure 8. Perspective view of the Chiaravalle Viaduct.

The aim of this study is to analyse a portion of the entire structure, that is the viaduct from the abutment A to the pier 13, where the continuous slab is interrupted by the expansion joint.

4.2 Seismic scenario and IM hazard curve

As introduced before, the parameters governing the seismic scenario (i.e., M , R , a , b , V_{S30}) are calibrated in order to provide an IM hazard curve consistent with that from NTC 2018 (Ministero

delle Infrastrutture e dei Trasporti 2018) for Chiaravalle.

For this purpose, it is assumed $m_0 = 4.5$, $m_{max} = 8$, $a = 4.5$ and $b=1$. The maximum epicentral distance is assumed equal to $r_{max} = 150$ km. The soil condition is described by the shear-wave velocity parameter $V_{S30} = 255$ m/s, representative of soil C condition according to Eurocode 8 (CEN 2004).

The spectral acceleration at the fundamental period of the system, $S_a(T)$, is chosen as IM for the purposes of the present study.

Figure 9 plots the IM hazard curve (blue line), obtained from Subset Simulation (performed on a damped linear elastic SDOF system with period $T = 0.62$ s and damping ratio $\xi=0.05$), with superimposed three different performance levels (coloured markers), identified by the im values with return period: 50 years, 475 years and 975 years. It is worth to note that the value of the period used for conditioning the IM is 0.62 s, as well as the value of the fundamental period of the bridge (corresponding to the transversal mode of vibration).

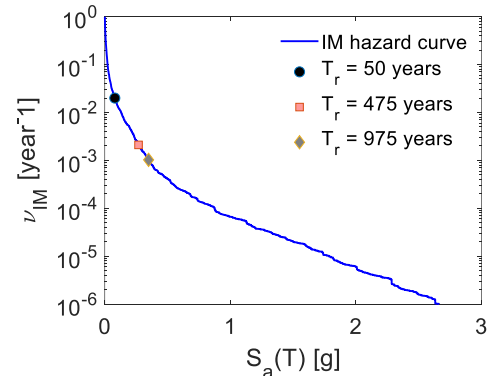
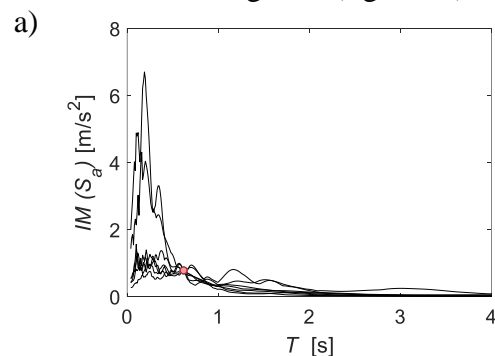


Figure 9. Hazard curve for $S_a(T)$ with three performance levels (limit states) highlighted.

For sake of completeness, from Figure 10 to Figure 12, the response spectra conditional to the three aforesaid performance hazard levels are shown (figures a), together with a set of conditional stochastic accelerograms (figures b).



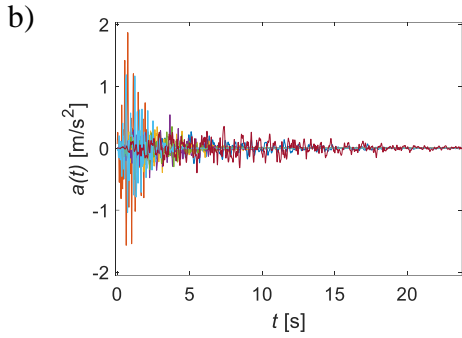


Figure 10. a) Response spectra conditional to the return period 50 years and b) corresponding set of 7 accelerograms.

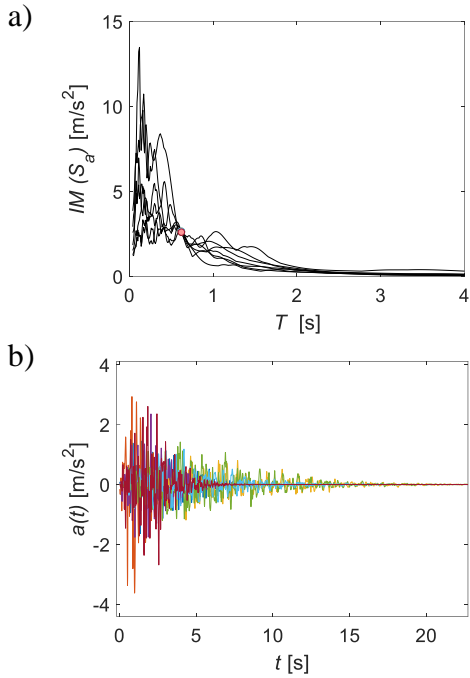


Figure 11. a) Response spectra conditional to the return period 475 years and b) corresponding set of 7 accelerograms.

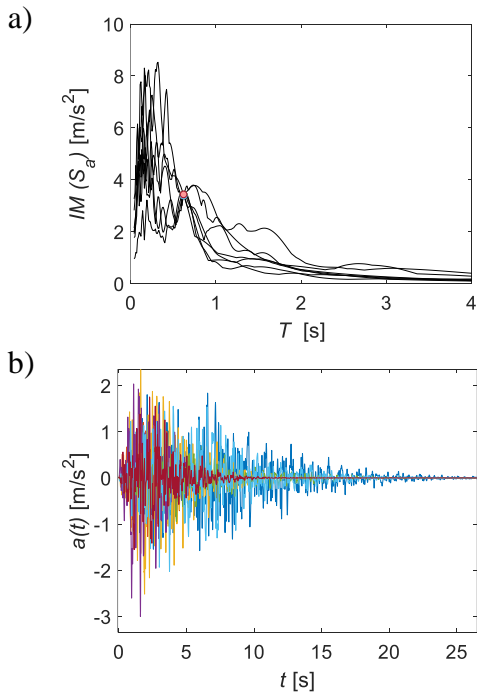


Figure 12. a) Response spectra conditional to the return period 975 years and b) corresponding set of 7 accelerograms.

Following the procedure described in (Scozzese et al 2019), the IM hazard curve is discretised in 20 intervals, identifying the 21 IM stripes adopted to perform MSA, as shown in Figure 13.

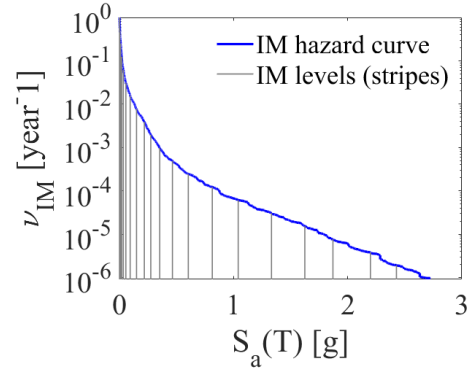


Figure 13. Hazard curve for $S_a(T_1)$ with highlighted the discretisation in IM levels used for MSA.

4.3 Numerical model

A three-dimensional nonlinear numerical model of the Chiaravalle viaduct is developed in OpenSees (McKenna et al. 2015). Deck girders are modelled as elastic beam-column elements, since they are expected to remain elastic in occurrence of seismic excitation. Force-based beam-column elements with reinforced concrete fiber section are adopted for the links, in order to catch the bar stress state. Bearings are modelled as elastic springs working in the longitudinal and/or transverse direction according to the bearing scheme in Figure 7. Columns, assumed as fixed at their base, are modelled using force-based plastic-hinge elements (Scott and Ryan 2013) which are able to take into account the evolution of the plastic hinge at the base of the pier. The pier section, a circular reinforced concrete discretised fiber section, is built so that effects of the confinement are considered according to (Mander 1988). Soil-structure interaction involving abutments or piers is neglected. Geometry and material properties adopted for the entire model are directly derived from the original design project of the viaduct.

4.4 Probabilistic analysis

Following the procedure described in (Scozzese et al 2019), MSA are performed by running 20 nonlinear time-history analyses at each of the 21 IM levels (up to $S_a(T)$ values close to 3.0g).

A selection of preliminary results from MSA is reported below.

In Figure 14 the evolution with the IM of the seismic demand expressed in terms of the

maximum base shear (along the transversal direction) under Pier n. 13 can be observed. In particular, the outcomes from each analysis are shown with blue circles, while the median trend of the EDP-IM relationship is superimposed with a red solid line.

It can be observed how both the demand intensity and the relevant dispersion increase by moving towards higher IMs.

Similarly, in Figure 15, it is shown the response at multiple IM level of the maximum stress on the steel bars (σ_{bar}) of the Link located above Pier n. 12.

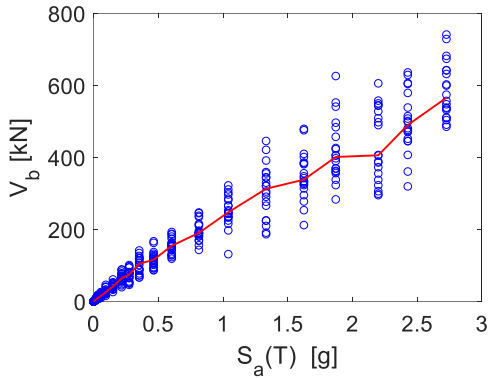


Figure 14. EDP-IM relationship for the maximum base shear (V_b along the transversal direction) monitored on Pier n. 13.

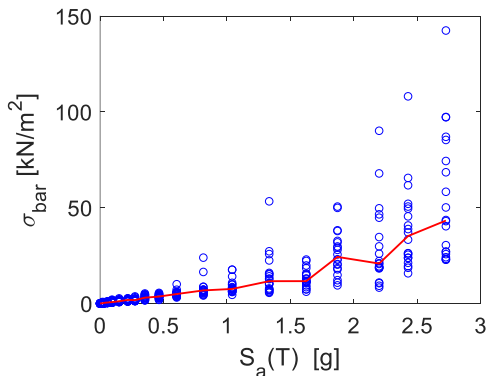


Figure 15. EDP-IM relationship for the maximum stress on the steel bars (σ_{bar}) of the Link on Pier n. 12.

In Figure 16 a comparison between the EDP-IM median trends of V_b of different piers is furnished, by using different colours to identify different piers. The trends are quite similar to each other, although lower shear values can be observed on Pier n. 13, which is located at the free end of the bridge.

For sake of completeness, in Figure 17, a comparison between the median trends of the maximum stress observed on the steel bars (σ_{bar}) of different links is provided. Unlike the case of shears, the demand values seem to increase by moving from the pier closest to the abutment (i.e., Link Pier 1) to the free end of the bridge (i.e., Link Pier 12).

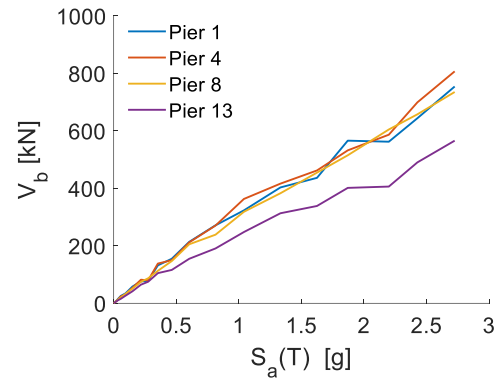


Figure 16. Comparison of the EDP-IM median trends for the maximum base shear (V_b) of different Piers.

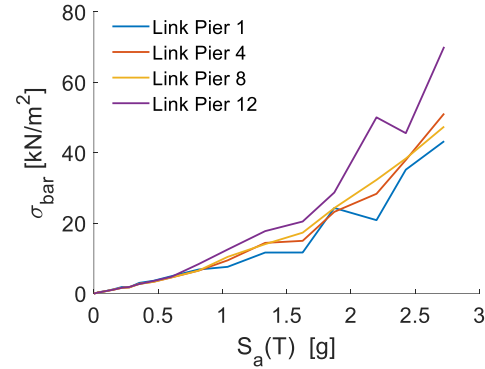


Figure 17. Comparison of the EDP-IM median trends for the maximum stress on the steel bars (σ_{bar}) of different Links.

5 CONCLUSIONS

In this paper, as a preliminary study towards the seismic fragility classification of the Italian bridge heritage, probabilistic analyses are performed on a real case study representative of a widespread class of Italian reinforced concrete bridges: the Chiaravalle viaduct, located in Central Italy, a multi-span precast bridge with a continuous slab on the top of the girders. The link slab represents, in addition to the classical response parameters relevant to the bridge components, one of the principal structural elements to be monitored, since its vulnerability has not been investigated in the literature.

The viaduct is entirely characterized by a reinforced concrete structure, with a link slab on simply supported V-shaped girders.

First, the numerical model is developed in order to capture the failure mechanisms most likely to occur, and then a probabilistic assessment of the seismic response of the bridge is carried out by performing multiple stripe analysis (MSA), providing a preliminary interpretation of the results on the main EDPs evaluating both ductile and fragile damage and failure mechanisms.

The probabilistic framework and finite element model developed in this paper will be used in future studies to provide a set of fragility curves accounting for all the relevant demand parameters and limit states.

REFERENCES

- Atkinson, G. M., Silva, W., 2000. Stochastic modeling of California ground motions, *Bulletin of the Seismological Society of America*, **90**(2), 255-274.
- Au, S.K., Beck, J.L., 2003. Subset simulation and its application to seismic risk based on dynamic analysis, *Journal of Engineering Mechanics*, **129**(8), 901-917.
- Boore, D.M., 2003. Simulation of ground motion using the stochastic method. *Pure and applied geophysics*, **160**(3-4), 635-676.
- Boore, D.M., Joyner, W.B., 1997. Site amplifications for generic rock sites. *Bulletin of the seismological society of America*, **87**(2), 327-341.
- Borzi, B., Ceresa, P., Franchin, P., Noto, F., Calvi, G. M., & Pinto, P. E., 2015. Seismic vulnerability of the Italian roadway bridge stock. *Earthquake Spectra*, **31**(4), 2137-2161.
- Calvi, G.M., 2004. Recent experience and innovative approaches in design and assessment of bridges. *13th World Conference on Earthquake Engineering*, August 1-6, Vancouver, Canada.
- Caner, A., Dogan, E., Zia, P., 2002. Seismic performance of multisimple-span bridges retrofitted with link slabs. *Journal of Bridge Engineering*, **7**(2), 85-93.
- Caner, A., Zia, P., 1998. Behavior and design of link slabs for jointless bridge decks. *PCI journal*, **43**, 68-81.
- CEN, 2004. Eurocode 8 - Design of structures for earthquake resistance: EN 1998-1 - Part 1: General rules, seismic actions and rules for buildings.
- Dall'Asta, A., Scozzese, F., Ragni, L., Tubaldi, E., 2017. Effect of the damper property variability on the seismic reliability of linear systems equipped with viscous dampers. *Bulletin of Earthquake Engineering*, **15**(11), 5025-5053.
- Di Sarno, L., da Porto, F., Guerrini, G., Calvi, P.M., Camata, G., Prota, A., 2018. Seismic performance of bridges during the 2016 Central Italy earthquakes. *Bulletin of Earthquake Engineering*, 1-33.
- EQE, 1994. The January 17, 1994 Northridge, California earthquake: an EQE summary report.
- EQE, 1995. The January 17, 1995 Kobe earthquake: an EQE summary report.
- European Committee for Standardization, Eurocode 8: *Design of structures for earthquake resistance - Part 1: General rules, seismic actions and rules for buildings*. EN 1998-1, December 2004.
- FEMA, 2003. HAZUS-MH MR1: Technical Manual, Federal Emergency Management Agency, Washington, DC.
- Itani, A.M., Bruneau, M., Carden, L., Buckle, I.G., 2004. Seismic Behavior of Steel Girder Bridge Superstructures. *Journal of Bridge Engineering*, **9**(3), 243-249.
- Jalayer, F., Beck, J.L., 2008. Effects of two alternative representations of ground-motion uncertainty on probabilistic seismic demand assessment of structures. *Earthquake Engineering & Structural Dynamics*, **37**(1), 61-79.
- Jalayer, F., Cornell, C.A., 2009. Alternative non-linear demand estimation methods for probability-based seismic assessments, *Earthquake Engineering & Structural Dynamics*, **38**(8), 951-972.
- Kaiser, A., Holden, C., Beavan, J., Beetham, D., Benites, R., Celentano, A., ... & Denys, P., 2012. The Mw 6.2 Christchurch earthquake of February 2011: preliminary report. *New Zealand journal of geology and geophysics*, **55**(1), 67-90.
- Karim, K.R., Yamazaki, F., 2003. A simplified method of constructing fragility curves for highway bridges. *Earthquake Engineering and Structural Dynamics*, **32**, 1603-1626.
- Kawashima, K., 2010. Seismic damage in the past earthquakes, seismic design of urban infrastructure. Lecture note, http://seismic.cv.titech.ac.jp/en/lecture/seismic_design/.
- Kramer, S.L., 2003. *Geotechnical Earthquake Engineering*, Prentice-Hall: Englewood Cliffs, NJ.
- Mander, J.B., Priestley, M.J., Park, R., 1988. Theoretical stress-strain model for confined concrete. *Journal of structural engineering*, **114**(8), 1804-1826.
- McKeena, F., Fenves, G., Scott, M., 2015. Open System for Earthquake Engineering Simulation (OpenSees). *Pacific Earthquake Engineering Research Center (PEER)*, University of California: Berkeley, CA.
- Ministero delle Infrastrutture e dei Trasporti, D.M.17.01.2018, *Aggiornamento delle "Norme Tecniche per le Costruzioni"*, G.U. n.42, 20.02.2018 (in Italian).
- Nielson, B.G., DesRoches, R., 2007. Seismic fragility methodology for highway bridges using a component level approach. *Earthquake Engineering & Structural Dynamics*, **36**(6), 823-839.
- Padgett, J.E., DesRoches, R., 2008. Methodology for the development of analytical fragility curves for retrofitted bridges. *Earthquake Engineering and Structural Dynamics*, **37**, 1157-1174.
- Pinto, P. E., Franchin, P., 2010. Issues in the upgrade of Italian highway structures. *Journal of Earthquake Engineering*, **14**, 1221-1252.
- Pinto, P.E., Giannini, R., Franchin, P., 2004. *Seismic reliability analysis of structures*, IUSS Press.
- Pitilakis, K., 2011. Systemic seismic vulnerability and risk analysis for buildings, lifeline networks and infrastructures safety gain. *European Collaborative research Project, Deliverable D3.6*. (FP7-ENV-2009-1-244061) <http://www.syner-g.eu>.
- Priestley, M.J.N., Calvi, G.M., Kowalsky, M.J., 2007. *Displacement-Based Seismic Design of Structures*, IUSS Press, Pavia, Italy. Scott, M.H., Ryan, K.L., 2013. Moment-Rotation Behavior of Force-Based Plastic Hinge Elements, *Earthquake Spectra*, **29**(2), 597-607.
- Scozzese, F., Dall'Asta, A., Tubaldi, E., 2019. Seismic risk sensitivity of structures equipped with anti-seismic devices with uncertain properties, *Structural Safety*, **77**, 30-47.
- Scozzese, F., Terracciano, G., Zona, A., Della Corte, G., Dall'Asta, A., Landolfo, R., 2018. Analysis of seismic non-structural damage in single-storey industrial steel buildings. *Soil Dynamics and Earthquake Engineering*, **114**, 505-519.
- Sevgili, G., Caner, A., 2009. Improved seismic response of multisimple-span skewed bridges retrofitted with link slabs. *Journal of Bridge Engineering*, **14**(6), 452-459.
- Tubaldi E., Barbato M, Dall'Asta A. 2012. Influence of model parameter uncertainty on transverse response and vulnerability of steel-concrete composite bridges with

dual load path. *ASCE Journal of Structural Engineering*, **138**(3), 363-374.

Tubaldi, E., Dall'Asta, A., 2012. Transverse free vibrations of continuous bridges with abutment restraint. *Earthquake Engineering and Structural Dynamics*, **41**(9), 1319–1340.